Indian Journal of Biochemistry & Biophysics
Vol. 62, June 2025, pp. 584-595
DOI: 10.56042/ijbb.v62i6.9056

Exploring benzothiazole derivatives: Promising PLK1 Inhibitors for cancer therapy through Virtual screening, Molecular docking, and ADMET evaluation

Shivkant Patel*, Ashish Shah & Ashim Kumar Sen

Department of Pharmacy, Sumandeep Vidyapeeth Deemed to be University, Piparia, Vadodara-391 760, Gujarat, India

Received 24 February 2024; *revised 05 March 2025*

The search for effective cancer therapies has driven significant interest in targeting Polo-like kinase 1 (PLK1), a crucial regulator of cell cycle progression, mitosis, epithelial-mesenchymal transition, autophagy, and DNA replication. Over expression of PLK1 is frequently observed in various cancers, making it a promising therapeutic target. Given the need for novel and potent PLK1 inhibitors, this study investigates the benzothiazole-containing drug 5f-203, known for inducing cell cycle arrest, as a potential PLK1 inhibitor. Using the PubChem database, novel PLK1 inhibitors were identified with 5f-203 (clinical trial, Phase 1) as the reference molecule. A comprehensive computational approach, including virtual screening, ligand and protein preparation, grid building, and molecular docking, was employed to evaluate co-crystallized ligand 5f-203, screened molecules, and newly designed compounds (N1-N6). Protein validation using ProSA (-7.9), ERRAT (95.36%), and the Ramachandran plot (84.1% residues in favored regions) confirmed model reliability. Lipinski's rule was applied as an additional filter, and molecular docking revealed binding affinity values ranging from -8.82 to -7.73 kcal/mol, with molecule P1 exhibiting the highest affinity (-8.82 kcal/mol). Interaction analysis showed that 5f-203 formed H-bonds with Arg120 and NH_2, while Ala66, Arg122, and Ile118 contributed to pi-alkyl interactions. Newly designed compounds (N1-N6) outperformed 5f-203 in docking scores, with synthetic accessibility below 4.5. ADMET studies further supported their drug-like potential. These findings suggest that the top 10 screened hits and newly designed benzothiazole derivatives hold promise as PLK1 inhibitors, offering a potential avenue for cancer therapy.

Keywords: 5f-203, Adsorption, Anti-cancer agents, Benzothiazole, Distribution, Docking, Excretion, Lipinski rule, Metabolism, Polo like kinase1 (PLK1)

Cancer is characterized by uncontrolled cell proliferation. It is regarded as the most fatal and common causes of death globally[1,2]. The most recent data from the International Agency for Research on Cancer, released on December 14, 2020, indicated that in 2020, there were 19.3 million new cases of cancer and 10 million fatalities worldwide. Additionally, the WHO forecasts a rise in cancer cases, estimating 29.5 million new diagnoses and 16.4 million deaths by 2040[3,4]. The identification of cancer therapies and associated targets has received a great deal of attention. The development of chemotherapeutic medications that target proteins that control the cell cycle has made significant progress[5-7]. Many malignancies are characterized by cell cycle disruption. In addition to disrupting the cell cycle, PLK1 drives cancer progression by reshaping cellular metabolism, specifically by boosting the pentose phosphate pathway and channelling glucose towards pathways involved in synthesizing macromolecules[8]. Inhibiting PLK1 expression often leads to decreased proliferation across various cancer cell types, establishing it as a potent proto-oncogene and a promising target for cancer therapy[9,10]. Currently, over ten PLK1 inhibitors (PLK1) are in clinical trials, with the FDA-approved kinase domain inhibitor volasertib (BI 6727) recognized as a "breakthrough therapy" in 2013[11,12]. The PLK family comprises serine/tyrosine kinase proteins, from PLK1 to Plk5, found widely in eukaryotic cells, exerting pivotal roles in diverse cell cycle stages. PLK1, the most extensively studied member, shares structural similarities with other kinases, featuring an N-terminal Ser/Thr kinase domain and a C-terminal polo-box domain repetition. Following a thorough review of the literature, it was discovered that certain benzothiazole derivatives exhibit encouraging anti-cancer properties. Among these, 5f-203 (IUPAC Name provided in Supplementary data) stands out as a significant drug. Acting as an Aryl hydrocarbon receptor (Ahr) agonist, it triggers a signalling cascade that leads to DNA damage and apoptosis in cancer

*Correspondence:
E-mail: shivapatel2609@gmail.com
Suppl. Data available on respective page of NOPR

cells susceptible to its cytotoxic effects. This drug is currently in clinical trial phase 1[13]. Apart from 5f-203, GW 610 (Fig. 1), are other benzothiazole derivatives which shows anti-cancer activity published in the literature[14-17]. Figure 1 displays the benzothiazole compounds available in the market, demonstrating their efficacy across a spectrum of diseases like Frentizole functions as both an antiviral and immunosuppressive agent. Riluzole is used in Amyotrophic Lateral Sclerosis, Thioflavin T is utilized for histological staining and biophysical investigations related to protein aggregation studies and Ethoxzolamide is employed for treating glaucoma, duodenal ulcers, and as a diuretic[18-21]. In this respect, we report structure based virtual screening studies of the "PubChem" using 5f-203 as rational molecule, followed by docking of 5f-203, screened molecules and newly designed molecules on Plk1 protein. The process of molecular docking involves ligand in 3-dimensional structure into receptor and variety of interaction positions on different sites was analysed. This approach is useful in drug development and therapeutic chemistry since it provides information about molecular recognition[22]. Ten promising compounds were selected through molecular docking and binding affinity analyses. These compounds exhibit potential as lead candidates in the exploration of potent PLK1 inhibitors during research and development.

Experimental approach and methodology

Choosing and Preparing Protein

Polo-like kinase 1 structure (PDB ID: 3DBE)[23] was taken from the data bank ofprotein[24]. Protein structure was downloaded in.PDB format. Utilizing an MMFF94 force field, this protein was made ready to the docking process through eliminating heteroatoms (water and ions), introducing polar hydrogen, and assigning Kollman charges.

Preparation of Pubchem database compounds and the reference ligand

PubChem serves as a publicly accessible molecular information repository, constituting a vital component of the NIH Roadmap Initiative's scientific endeavors. Within its extensive dataset, PubChem hosts approximately twenty-seven million entries encompassing diverse chemical structures derived from over seventy million substance depositions. Furthermore, it contains nearly 449, 000 bioassay recordings, encompassing a wide array of *in vitro* metabolic and cell-based screening bioassays targeting over seven thousand genes and proteins

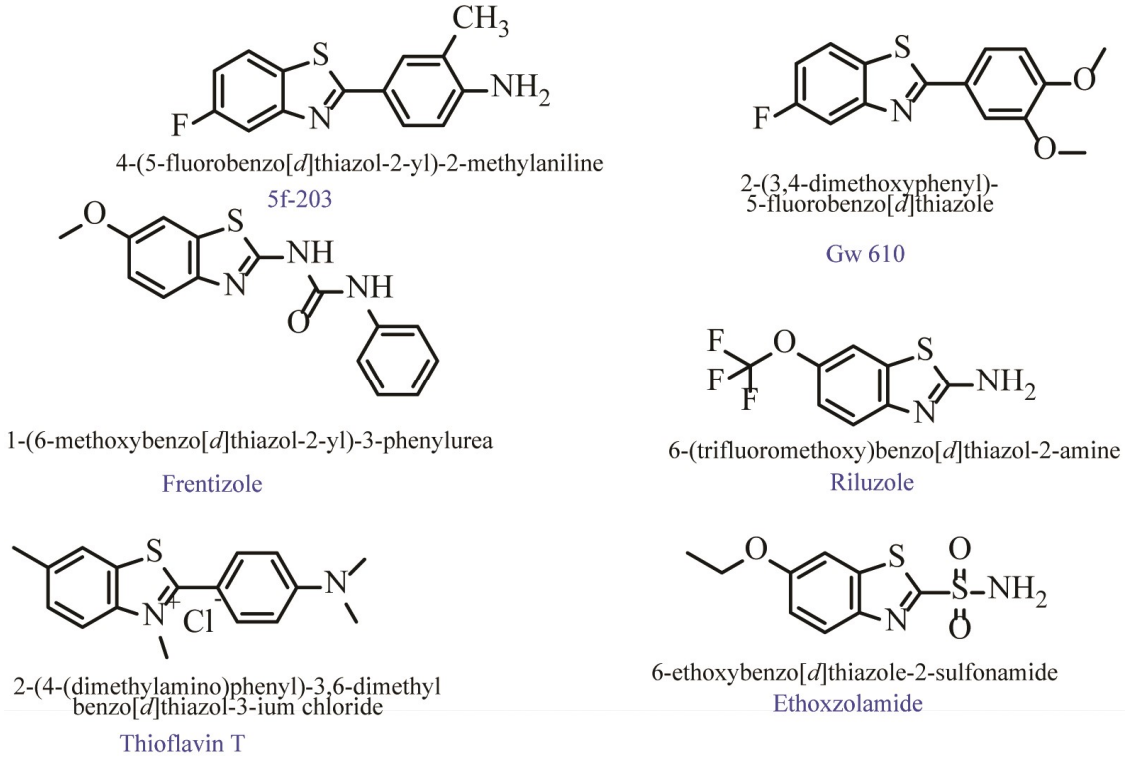

Fig. 1 — 2D structures of benzothiazole derivatives and marketed drugs

associated with more than 1.8 million molecules[25]. In drug development, virtual screening techniques are commonly utilized to streamline processes and conserve resources. PubChem provides comprehensive molecular data including information on attributes such as the molecular weight, computed log P, number of hydrogen-bond donors and acceptors and count of rotatable bonds. For the virtual screening process, 5f-203 was selected as the reference molecule, resulting in the identification of 1144 potential candidates. The 2D and 3D chemical structures of benzothiazole-containing compounds were retrieved from the PubChem website in sdf and Mol formats. Subsequently, these structures were converted into pdb files using Pyrx and further transformed into pdbqt format using the autodock tools ligand preparation module 1.5.7[26-28].

Generation of grid and molecular docking

The active region of a protein that was identified through the protein-ligand interactions profiler website is displayed in supplementary data as (Fig. 1)[29]. The identified residues were utilized to build a grid box surrounding the active site. AutoDock utilizes Autogrid 4.0 to generate interaction energy grid maps (A, C, Cl, NA, OA, N, and HD) corresponding to various molecular types present in ligands[30]. The interacting residues obtained from PLIP are employed to define a grid box surrounding the target site. The grid centre coordinates are set at 16.285 for x, 79.163 for y, and 46.04 for z dimensions, while the grid box dimensions are adjusted to 50 grid points each to encompass all amino acid residues within the active pocket, with a spacing of 0.375 Å between grid points. Discovery Studio visualizer[31] and Autodock tools 1.5.6[32,33] was employed to assess and display the docking findings.

ADMET prediction and Lipinski's rule of 5

To guarantee that the newly developed scaffolds possess crucial physiological efficacy and pharmacokinetic characteristics suitable for therapeutic purposes, Swiss ADME prediction was employed to evaluate parameters including iLOGP (Log Po/w), number of rotatable bonds, molecular weight, gastric absorption, hydrogen bond acceptors and donors, topological polar surface area (TPSA). Additionally, the PreADME-T server was utilized to assess inhibitory potential of screened compounds on cytochrome P450 enzymes, carcinogenicity and the plasma protein binding[34,35].

Results and Discussion

Choosing and preparing protein

The crystal structure of the "Polo-like-kinase1 domain complexed with Compound 557" (PDB: 3DBE) at a resolution of 3.32Å was utilized, obtained from the Protein Data Bank website[36]. After adding atoms and missing residues, hydrogen atoms were incorporated and water molecules were removed. The protein structure was subjected to a reduction process employing 500 steps of the conjugate gradient technique to ensure compatibility for docking. Various validation methods were conducted to assess the model's quality, as detailed in (Table 1 and Fig. 2). Ramachandran analysis revealed no Amino acid residues in the outlier region, with 92.1% of Amino acid residues in the favored zone, 7.5% in the additionally allowed zone, and 0% in the outlier zone[37]. ProSA evaluation yielded a Z-score of -7.9, indicating a good match to NMR structural data[38]. Figure 2 displays results from the Ramachandran plot[39,40], ERRAT plot, and ProSA score. ERRAT plot depicts an error function of a 9-residue sliding window, assessing non-bonded interactions between specific atom types. The model's ability to meet criteria satisfactorily signifies its accuracy in representing the protein.

Database screening and ligand preparation

During structure-based virtual screening, 5f-203 served as the reference compound, resulting in the identification of 1144 molecules[41]. These molecules were downloaded from the database in SDF format and converted to Mol2 format. Energy minimization was then performed using the Open Babel program through the Pyrx (Python Prescription Virtual Screening) module[42,43]. Subsequently, the Raccoon program was employed to filter out compounds not compliant with the

Table 1 — Assessment of constructed protein model

Programs/ Parameters	Results
PROCHECK (Ramachandran Plot)	
Amino acid residues within the most preferred region	84.1% (207)
Amino acid residues within the regions of additional permissibility	13.8% (34)
Amino acid residues within the expansively permissible regions	2.0% (5)
Amino acid residues within the restricted or prohibited regions	0% (0)
ERRAT (Overall quality factor)	95.367%
ProSA (Z score)	-7.9

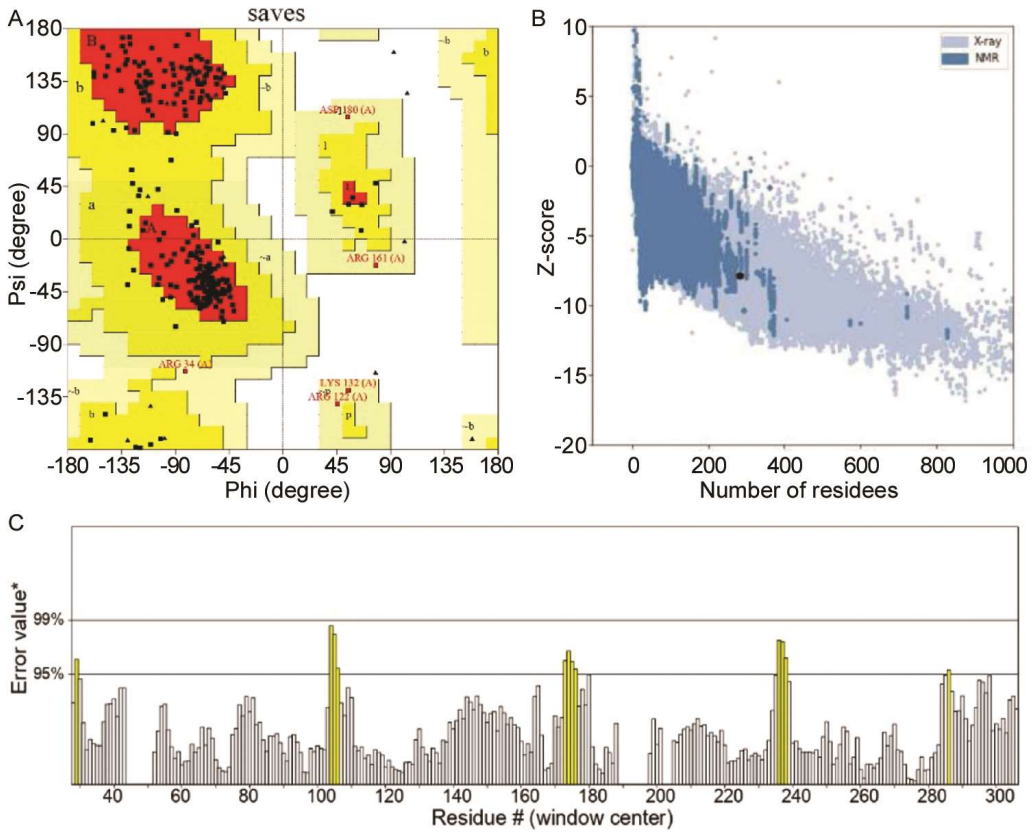

Fig. 2 — Validation Parameters (A) Ramachandran plot of Protein; (B) Z-score plot from ProSA –web of Protein; and (C) ERRAT plot of Protein

Lipinski rule of 5, reducing the number of compounds to 1031[44].

Generation of grid and molecular docking

A three-dimensional grid was built surrounding interacting residues, covering a distance of 5Å. These residues include Leu116, Val100, Glu117, Cys119, Ile118, Ala66, Leu116, Arg120, and Cys53. Compound 557 is a 2-amino-pyrazolopyridine derivative, was co-crystallized with the protein. After docking, the co-crystallized ligand was superimposed, resulting in an RMSD of less than 1 (Fig. S2 in supplementary materials). Subsequently, 5f-203 was docked onto the same grid box with a binding energy of -6.71 kcal/mol. This grid-based approach produced reliable results consistent with the interactions observed for the co-crystallized ligand before docking (Fig. 3). The docking analysis revealed a typical hydrogen bond formation between the -NH_2 group and Arg120 of compound 5f-203. Additionally, pi-alkyl interactions were observed with the amino acid residues Ala66, Arg122, and Ile118. Similar grid dimensions were utilized for docking both screened and newly designed molecules.

Molecular docking-based screening revealed a range of compound binding energies, with a mean of -6.71 kcal/mol. Among the top 10 hits, P1 exhibited the highest docking score (-8.82 kcal/mol) at the protein's active site, while P10 displayed the lowest score (-7.73 kcal/mol; see Table 2). P1 demonstrated hydrogen bonding interactions with Arg43 and Cys119, along with pi-sigma bonds with Leu45. Additionally, pi-alkyl interactions occurred with Val100, Phe169, and Leu116. A pi-sulfur bond was established with Cys53 and Cys11. Similar interaction patterns were observed for other compounds within the top 10 hits. For example, P2 formed a hydrogen bond with Arg43 and Cys119, as well as pi-sigma bonds with Leu45. P3 exhibited pi-alkyl interactions with Ala66, Arg122, and other residues, while P4 engaged in hydrogen bonding with Cys119 and Arg43, along with pi-sigma bonds with Leu45. These interactions continued with slight variations across P5-P10. Notably, P7 formed hydrogen bonds with Cys119 and Arg43, and exhibited pi-alkyl interactions

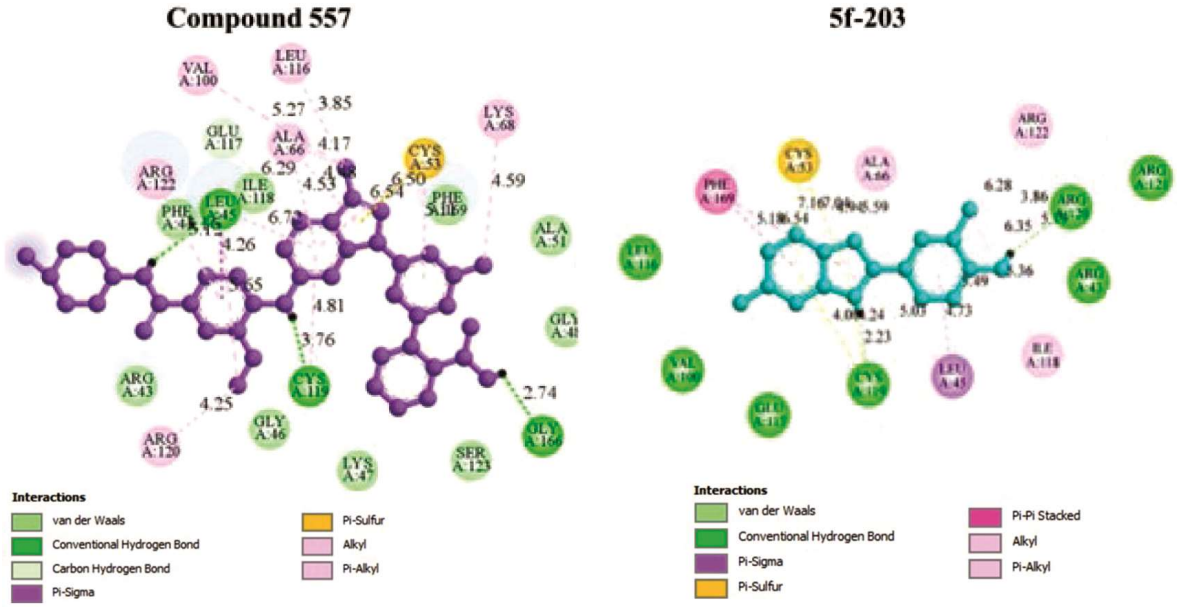

Fig. 3 — 2D interaction of Drug 5f-203 and Compound 557 in binding pocket of 3DBE protein

Table 2 — Identified compounds and standard drug (5f-203) docking score

C. No.	PubChem ID	Score in (Kcal/mol)
P1	10779701	-8.82
P2	10946124	-8.68
P3	153949097	-8.61
P4	15880521	-8.47
P5	137735789	-8.36
P6	15880522	-8.28
P7	10566560	-7.92
P8	10589414	-7.86
P9	159531422	-7.77
P10	10542666	-7.73
5f-203	-	-6.71

with Ala66 and Arg120. Additionally, P9 formed hydrogen bonds with Glu126, pi-sigma bonds with Leu45 and Arg120, and engaged in alkyl and pi-alkyl interactions with Leu125 and Phe169. Meanwhile, P10 displayed hydrogen bonds with Cys119 and Arg43, along with interactions with Glu117 and Ile118. Overall, these findings are summarized in (Table 2), while (Fig. 4) provides an overview of the molecular interactions of the top 10 hit molecules.

ADMET prediction and Lipinski's rule of 5

The assessment of Lipinski's rule of drug-likeness was conducted using the Swiss ADME prediction tool (http://www.swissdme.ch/). Additionally, the PreADMET server facilitated the prediction of ADMET attributes. Bioavailability, influenced by absorption location, was among the ADMET features evaluated. All compounds demonstrated inhibition of CYP1A2 and CYP2C19 enzymes. The toxicity profile of the compounds was established using two years' worth of data from the National Toxicology Program and the US Food and Drug Administration, focusing on mouse and rat exposure. Carcinogenicity studies in mice and rats revealed that compound P5 and P9 exhibited carcinogenic properties in mice, while the remaining compounds were non-carcinogenic in both mice and rats (see Table 3). Ease of synthesis was assessed, with a score less than 4.5 indicating favorable synthesis conditions.

A comprehensive overview of docking studies and new compound design

Based on the docking analysis of the screened compounds, crucial interactions were identified. Weak pi-alkyl bonds were observed at the second position of the benzothiazole ring, while hydrogen bonds were detected with various substitutions around the nitrogen atom. Leveraging this insight, six novel molecules were designed and subsequently docked with the same protein, resulting in docking scores of approximately -8 kcal/mol for all compounds (refer to Table 4).

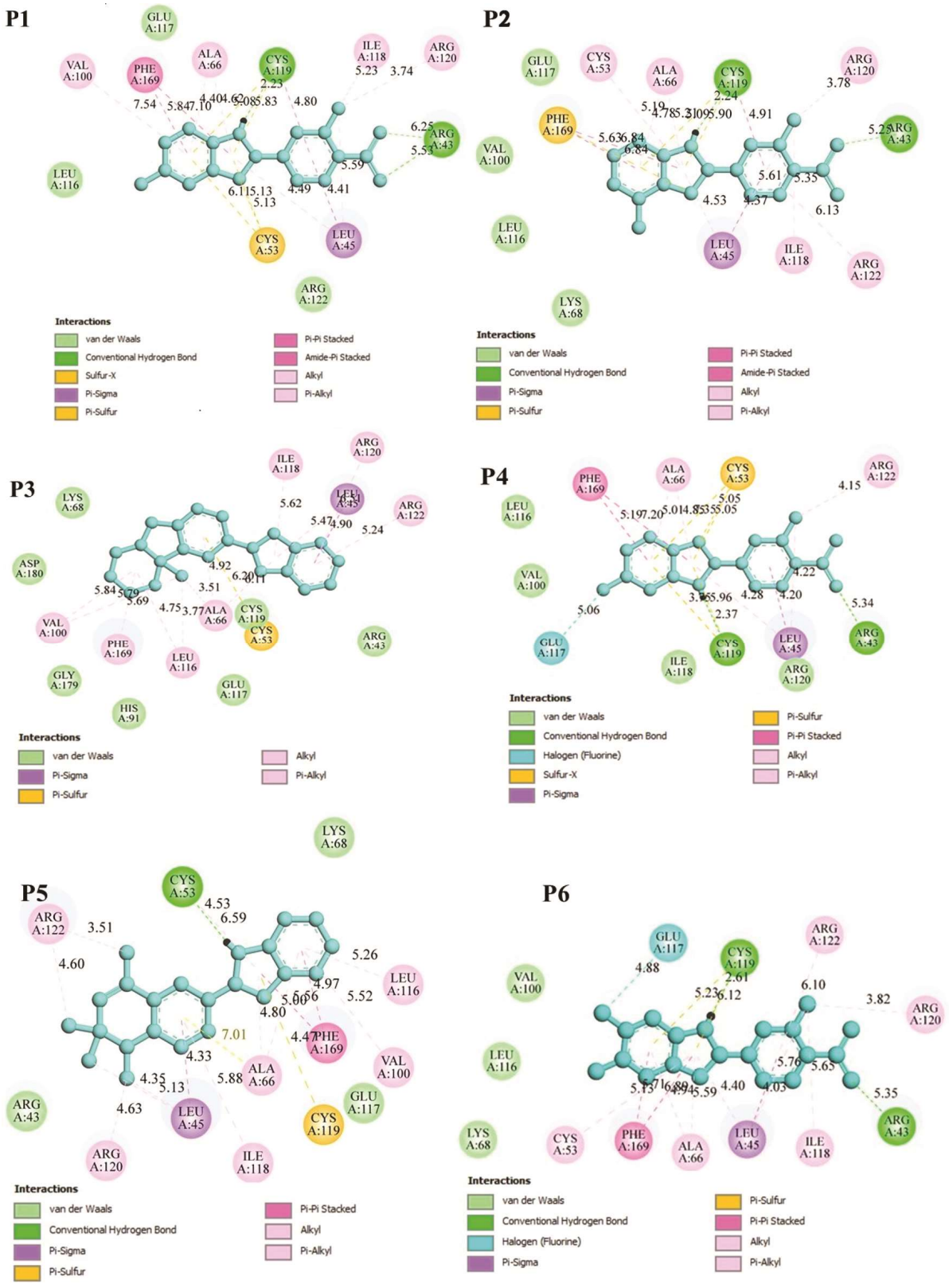
P1
GLU A:117
VAL A:100
PHE A:169
ALA A:66
CYS A:119
ILE A:118
ARG A:120
ARG A:43
LEU A:116
CYS A:53
LEU A:45
ARG A:122
Interactions
van der Waals
Conventional Hydrogen Bond
Sulfur-X
Pi-Sigma
Pi-Sulfur
Pi-Pi Stacked
Amide-Pi Stacked
Alkyl
Pi-Alkyl
P2
GLU A:117
CYS A:53
ALA A:66
CYS A:119
ARG A:120
PHE A:169
ARG A:43
VAL A:100
LEU A:116
LEU A:45
ILE A:118
ARG A:122
LYS A:68
Interactions
van der Waals
Conventional Hydrogen Bond
Pi-Sigma
Pi-Sulfur
Pi-Pi Stacked
Amide-Pi Stacked
Alkyl
Pi-Alkyl
P3
ILE A:118
ARG A:120
LYS A:68
LEU A:45
ARG A:122
ASP A:180
VAL A:100
ALA A:66
CYS A:119
CYS A:53
ARG A:43
PHE A:169
LEU A:116
GLY A:179
GLU A:117
HIS A:91
Interactions
van der Waals
Pi-Sigma
Pi-Sulfur
Alkyl
Pi-Alkyl
P4
PHE A:169
ALA A:66
CYS A:53
ARG A:122
LEU A:116
VAL A:100
GLU A:117
CYS A:119
LEU A:45
ILE A:118
ARG A:120
ARG A:43
Interactions
van der Waals
Conventional Hydrogen Bond
Halogen (Fluorine)
Sulfur-X
Pi-Sigma
Pi-Sulfur
Pi-Pi Stacked
Alkyl
Pi-Alkyl
LYS A:68
P5
CYS A:53
ARG A:122
LEU A:116
PHE A:169
VAL A:100
ALA A:66
GLU A:117
ARG A:43
LEU A:45
CYS A:119
ARG A:120
ILE A:118
Interactions
van der Waals
Conventional Hydrogen Bond
Pi-Sigma
Pi-Sulfur
Pi-Pi Stacked
Alkyl
Pi-Alkyl
P6
GLU A:117
ARG A:122
CYS A:119
VAL A:100
ARG A:120
LEU A:116
ARG A:43
LYS A:68
CYS A:53
PHE A:169
ALA A:66
LEU A:45
ILE A:118
Interactions
van der Waals
Conventional Hydrogen Bond
Halogen (Fluorine)
Pi-Sigma
Pi-Sulfur
Pi-Pi Stacked
Alkyl
Pi-Alkyl

(*Contd.*)

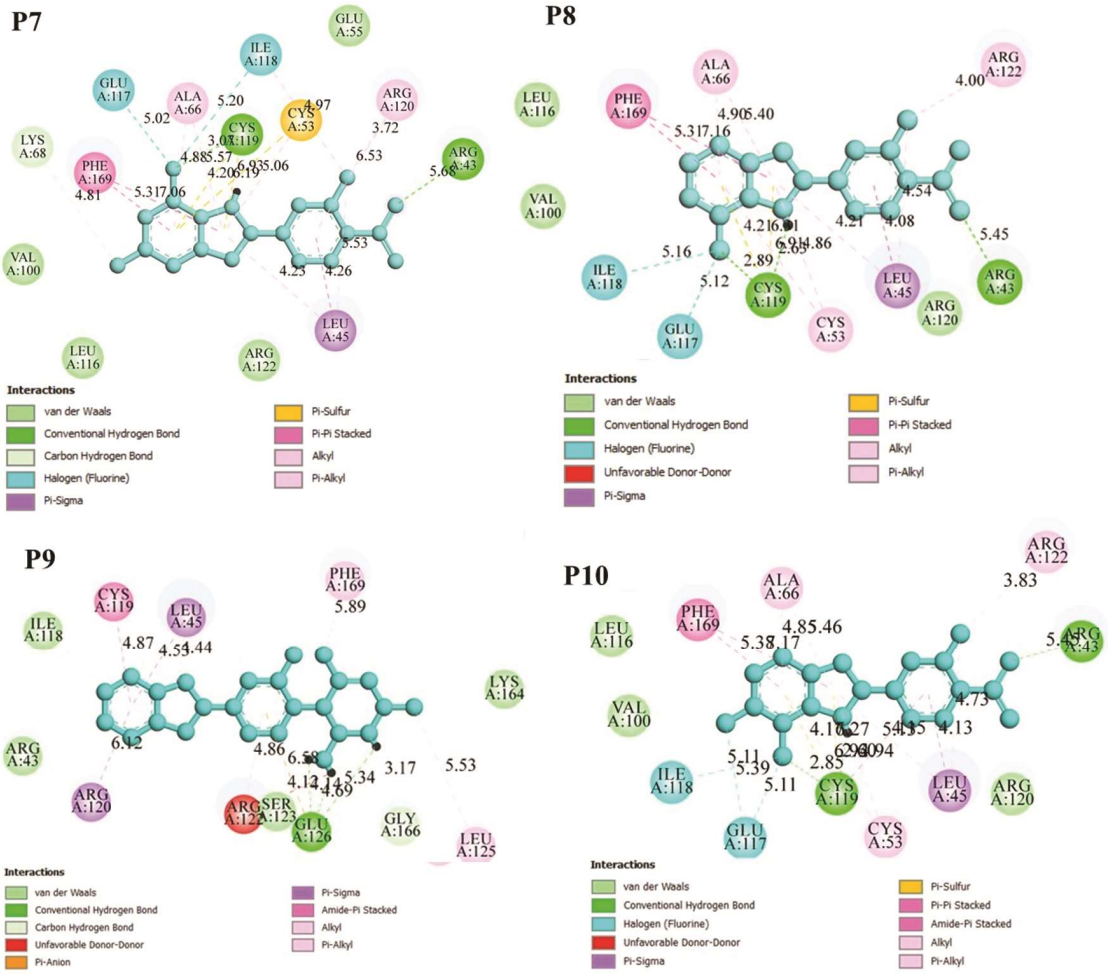

Fig. 4 — Docking 2D interactions of hit-molecules in active site

Table 3 — Top ten hit-molecules ADME-T and molecular pharmacokinetic and analysis from SwissADME and preADMET server

C. No.	MW ($gmol^{-1}$)	iLogP	HA	HD	NRB	TPSA ($Å^2$)	CYP2 C19 Inhibition	CYP1A2 Inhibition	CYP 3A4 Inhibition	GI absorption	Plasma Protein Binding (%)	Synthetic Accessibility	Carcinogenicity MOUSE	Carcinogenicity RAT
P1	288.3	2.68	4	0	2	86.95	Yes	Yes	No	High	90.91	2.74	-	-
P2	288.3	2.69	4	0	2	86.95	Yes	Yes	No	High	91.07	2.79	-	-
P3	318.44	3.54	2	0	1	53.49	Yes	Yes	Yes	High	94.19	3.81	-	-
P4	288.3	2.69	4	0	2	86.95	Yes	Yes	No	High	92.00	2.7	-	-
P5	320.45	3.7	1	0	1	44.37	Yes	Yes	No	High	99.36	3.46	+	-
P6	306.29	2.69	5	0	2	86.95	Yes	Yes	No	High	91.94	2.83	-	-
P7	306.29	2.66	5	0	2	86.95	Yes	Yes	No	High	91.26	2.8	-	-
P8	288.3	2.66	4	0	2	86.95	Yes	Yes	No	High	91.22	2.76	-	-
P9	348.46	3.74	3	1	2	82.75	Yes	Yes	Yes	High	80.69	4.21	+	-
P10	306.29	2.66	5	0	2	86.95	Yes	Yes	No	High	92.12	2.85	-	-

C.no.: Compound identification number; GI: Gastrointestinal Absorption; Plasma Protein Binding: Strongly Bound > 90% and Weekly bound < 90%, HD ≤ 5, iLOGP< 5, HA ≤ 10; Carcinogenicity:-: non-carcinogenic.+: carcinogenic (Lipophilicity) : -0.7< XLOGP3< + 5.0; MW: 150 g/mol< MV< 500 g/mol

Table 4 — Docking score of designed compounds

C. No.	Score in (Kcal/mol)
N1	-8.48
N2	-7.95
N3	-8.38
N4	-7.94
N5	-8.41
N6	-7.99

Docking studies showed similar results (see Fig. 5). Furthermore, considering ease of synthesis, the synthetic accessibility score for these molecules was determined to be less than 4.5 (see Table 5). Pharmacokinetic assessments indicated high gastrointestinal absorption for all compounds. Figures 6-8 illustrates the 2D structures of the designed molecules.

Table 5 — Physico-chemical Parameters and ADME-T analysis of Designed compounds

Properties	Factors	N1	N2	N3	N4	N5	N6
Physico-chemical properties	Formula	$C_{20}H_{19}FN_2S$	$C_{20}H_{19}FN_4S$	$C_{20}H_{19}FN_2S$	$C_{20}H_{19}FN_4S$	$C_{20}H_{18}F_2N_2S$	$C_{20}H1_8F_2N_4S$
	MW (g mol^{-1})	338.44	366.46	338.44	366.46	356.43	384.45
	Heavy atoms	24	26	24	26	25	27
	Arom. heavy atoms	15	15	15	15	15	15
	HA	2	4	2	4	3	5
	HD	0	1	0	1	0	1
	Molar refractivity	104.59	113.48	104.59	113.48	104.55	113.44
	TPSA (A^2)	44.37	82.75	44.37	82.75	44.37	82.75
Lipophilicity	log Po/w (XLOGP3)	5.13	3.89	5.13	3.89	5.23	3.99
Water solubility	log S (ESOL)	Insoluble	Insoluble	Insoluble	Insoluble	Insoluble	Insoluble
Drug likeness	Bioavailability Score	0.55	0.55	0.55	0.55	0.55	0.55
Medicinal Chemistry	Synthetic Accessibility	3.5	4.25	3.52	4.26	3.59	4.32
Carcinogenicity	Mouse	+	+	+	+	+	+
Carcinogenicity	Rat	-	-	-	-	-	-

Note: Abbreviations: same as Table 3 and POLAR (Polarity) 20Å^2< TPSA< 130 Å^2; -6 < Log S (ESOL) <0

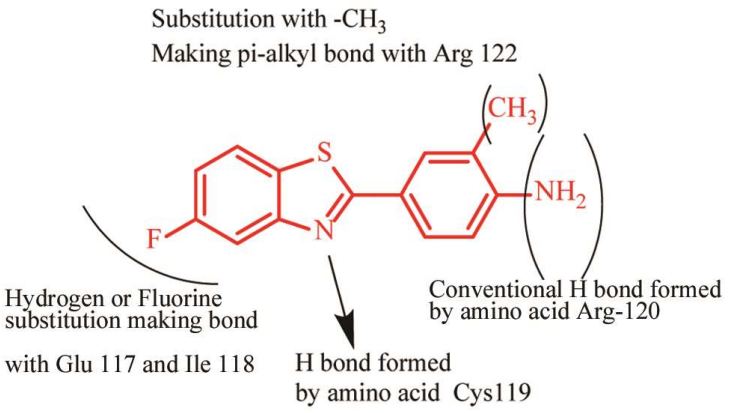

Fig. 5 — Summary of Docking Studies

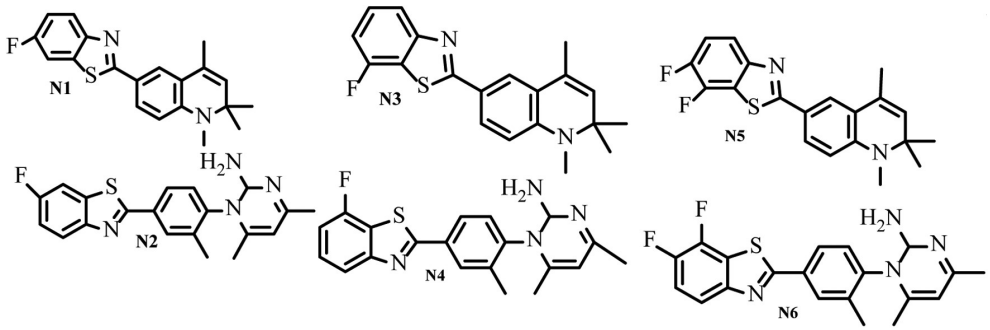

Fig. 6 — 2D Structures of Designed Compounds (N1-N6)

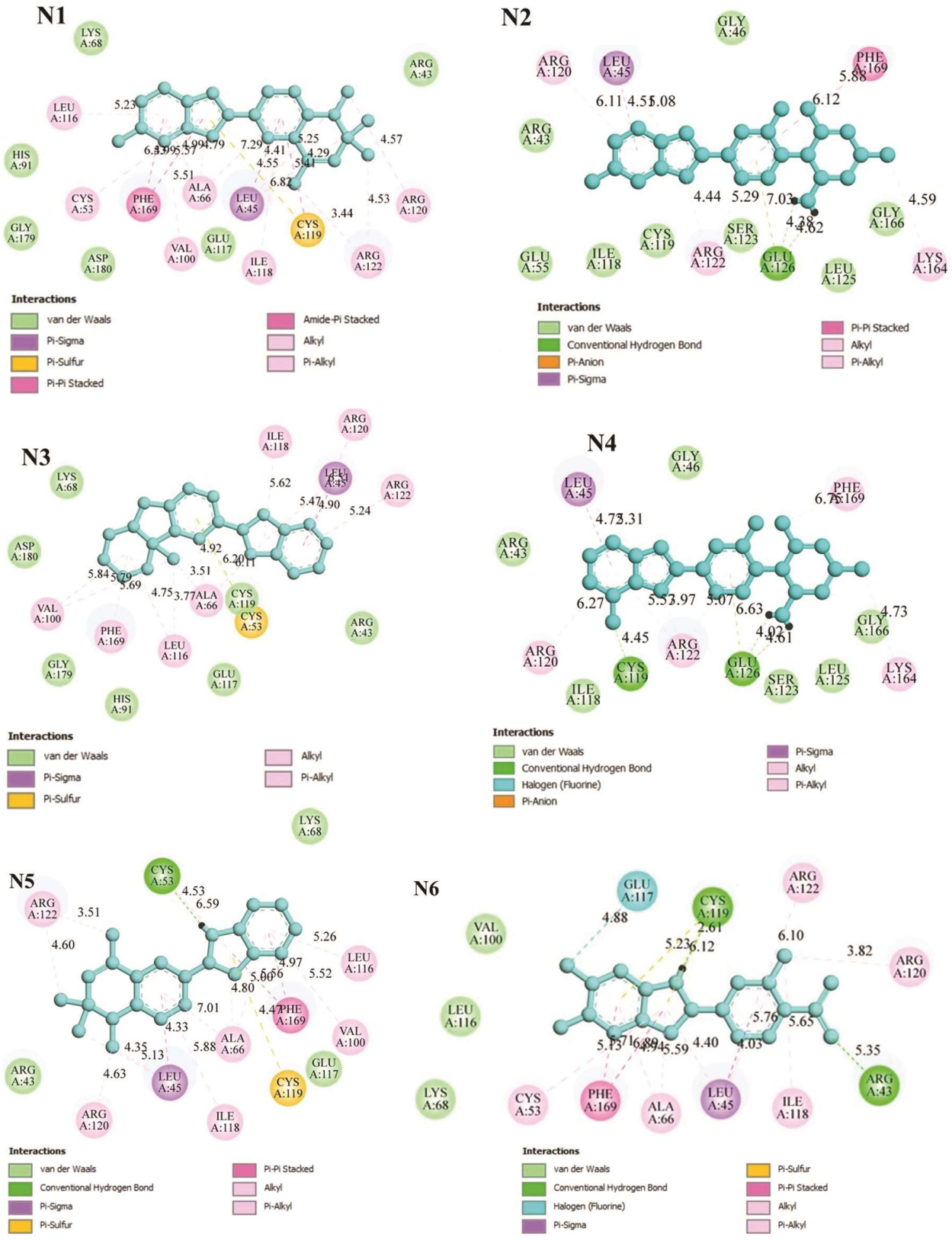

Fig. 7 — Molecular interactions of the designed molecules (N1-N6)

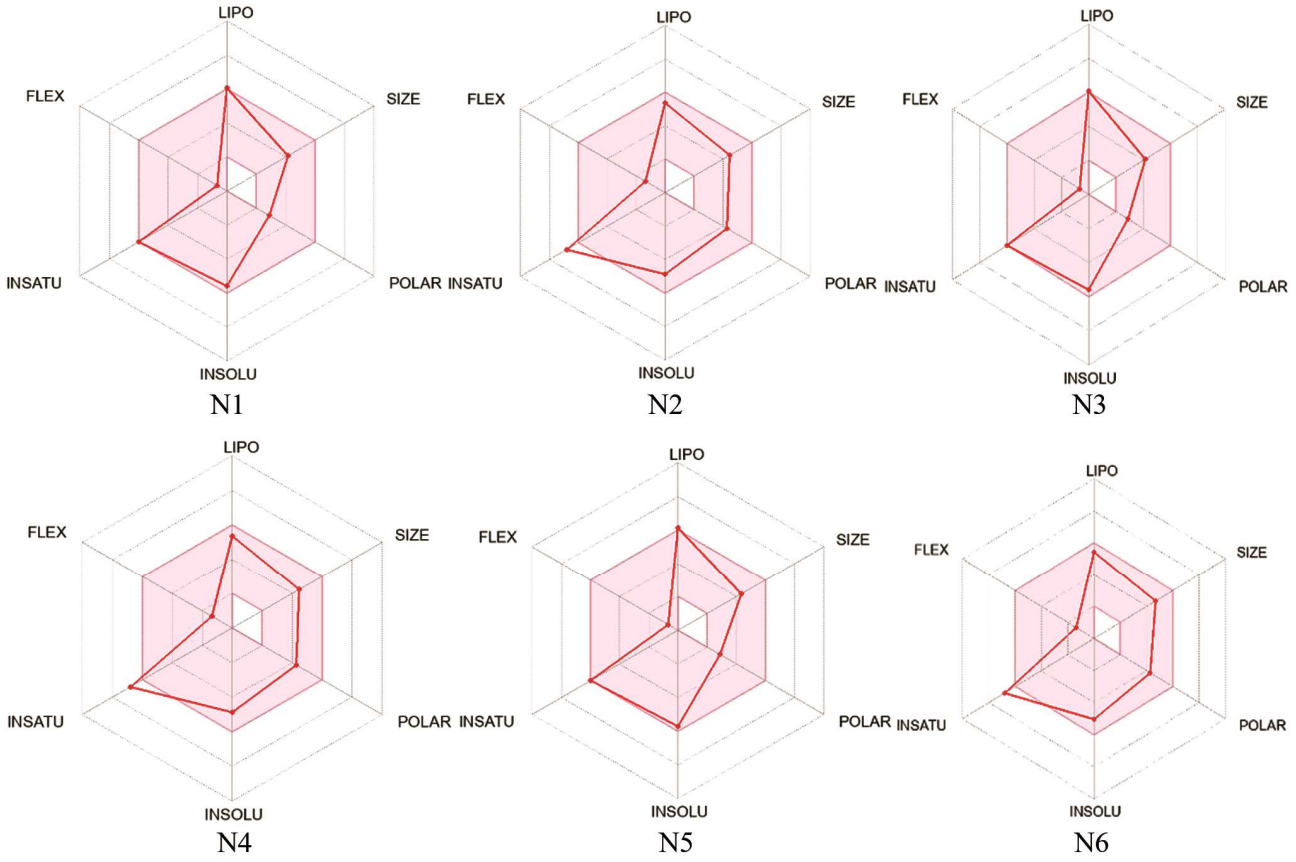

Fig. 8 — Designed molecules (N1-N6) ADMET properties generated by SwissADME

Conclusion

The "PubChem" database was employed for structure-based virtual screening to identify potential chemical entities as Plk1 inhibitors. Ten bioactive compounds showed higher docking scores than the reference ligand. Pharmacokinetic profiling indicated that these top 10 drugs do not inhibit the CYP2D6 enzyme, and most of them are non-carcinogenic. Utilizing the results from pharmacokinetic profiling, drug-likeness assessment, toxicity data, and docking studies, new compounds were designed and evaluated for their binding affinities. These newly designed compounds demonstrated docking scores surpassing that of 5f-203, with synthetic accessibility scores below 4.5. In summary, the integration of molecular docking studies, ADMET assessments, and considerations regarding ease of synthetic accessibility will facilitate the design of novel molecules targeting Plk1.

Acknowledgement

SP conceived and planned the research. Conducted protein preparation, molecular virtual screening, and docking research. AS done verification and ultimate approval of all results. AKS drafted the text and completed the findings. All writers authorized the final draft.

Conflict of interest

All authors declare no conflicts of interest.

References

1 Vineis P & Wild CP, Global cancer patterns: causes and prevention. *The Lancet*, 383 (2014) 549.

2 Organization W. H. (2020). WHO Report on Cancer: Setting Priorities, Investing Wisely and Providing Care for All. Geneve, Switzerland: WHO

3 Shah SC, Kayamba V, Peek Jr RM & Heimburger D, Cancer control in low-and middle-income countries, is it time to consider screening. *J Glob Onco*, 5 (2019) 1.

4 Sung H, Ferlay J, Siegel RL, Laversanne M, Soerjomataram I, Jemal A & Bray F, Global cancer statistics 2020: GLOBOCAN estimates of incidence and mortality worldwide for 36 cancers in 185 countries. *CA Cancer J Clin*, 71 (2021) 209.

5 Goyal L, Hingmire S & Parikh PM, Newer diagnostic methods in oncology. *Med J Armed Forces India*, 62 (2006) 162.

6 Charmsaz S, Prencipe M, Kiely M, Pidgeon GP & Collins DM, Innovative technologies changing cancer treatment. *Cancers*, 10 (2018) 208.

7 Pucci C, Martinelli C & Ciofani G, Innovative approaches for cancer treatment: current perspectives and new challenges. *Ecancermedicalscience*, 13 (2019) 961.

8 Ma X, Wang L, Huang D, Li Y, Yang D, Li T, Li F, Sun L, Wei H, He K & Yu F, Polo-like kinase 1 coordinates biosynthesis during cell cycle progression by directly activating pentose phosphate pathway. *Nat Commun*, 8 (2017) 1506.

9 Spänkuch-Schmitt B, Wolf G, Solbach C, Loibl S, Knecht R, Stegmüller M, von Minckwitz G, Kaufmann M & Strebhardt K, Downregulation of human polo-like kinase activity by antisense oligonucleotides induces growth inhibition in cancer cells. *Oncogene*, 21 (2002) 3162.

10 Gheghiani L, Wang L, Zhang Y, Moore XT, Zhang J, Smith SC, Tian Y, Wang L, Turner K, Jackson-Cook CK & Mukhopadhyay ND, PLK1 induces chromosomal instability and overrides cell-cycle checkpoints to drive tumorigenesis. *Cancer Res*, 81 (2021) 1293.

11 Rudolph D, Steegmaier M, Hoffmann M, Grauert M, Baum A, Quant J, Haslinger C, Garin-Chesa P & Adolf GR, BI 6727, a Polo-like kinase inhibitor with improved pharmacokinetic profile and broad antitumor activity. *Clin Cancer Res*, 15 (2009) 3094.

12 Gjertsen BT & Schöffski P, Discovery and development of the Polo-like kinase inhibitor volasertib in cancer therapy. *Leukemia*, 29 (2015) 1.

13 McLean LS, Watkins CN, Campbell P, Zylstra D, Rowland L, Amis LH, Scott L, Babb CE, Livingston WJ, Darwanto A & Davis Jr WL, Aryl hydrocarbon receptor ligand 5F 203 induces oxidative stress that triggers DNA damage in human breast cancer cells. *Chem Res Toxicol*, 28 (2015) 855.

14 Irfan A, Batool F, Zahra Naqvi SA, Islam A, Osman SM, Nocentini A, Alissa SA & Supuran CT, Benzothiazole derivatives as anticancer agents. *J Enzyme Inhib Med Chem*, 35 (2023) 265.

15 Pathak N, Rathi E, Kumar N, Kini SG & Rao CM, A review on anticancer potentials of benzothiazole derivatives. *Mini Rev Med Chem*, 20 (2020) 12.

16 Tariq S, Kamboj P & Amir M, Therapeutic advancement of benzothiazole derivatives in the last decennial period. *Arch Pharm,* 352 (2018) 1800170.

17 Sulthana S & Pandian P, A review on Indole and Benzothiazole derivatives its importance. *J Drug Deliv Ther*, 9 (2019) 505.

18 Xie Y, Deng S, Chen Z, Yan S & Landry DW, Identification of small-molecule inhibitors of the Aβ–ABAD interaction. *Bioorg Med Chem Lett*, 16 (2006) 4657.

19 Aiken CB, Pramipexole in psychiatry: a systematic review of the literature. *J Clin Psychiatry*, 68 (2007) 1230.

20 Xue C, Lin TY, Chang D & Guo Z, Thioflavin T as an amyloid dye: fibril quantification, optimal concentration and effect on aggregation. *R Soc Open Sci*, 4 (2017) 160696.

21 Mincione F, Scozzafava A & Supuran CT, The development of topically acting carbonic anhydrase inhibitors as antiglaucoma agents. *Curr Top Med Chem*, 7 (2007) 849.

22 Stanzione F, Giangreco I & Cole JC, Use of molecular docking computational tools in drug discovery. *Prog Med Chem*, 60 (2021) 273.

23 Fucini RV, Hanan EJ, Romanowski MJ, Elling RA, Lew W, Barr KJ, Zhu J, Yoburn JC, Liu Y, Fahr BT & Fan J, Design and synthesis of 2-amino-pyrazolopyridines as Polo-like kinase 1 inhibitors. *Bioorg Med Chem Lett*, 18 (2008) 5648.

24 Berman HM, Westbrook J, Feng Z, Gilliland G, Bhat TN, Weissig H, Shindyalov IN & Bourne PE, The protein data bank. *Nucleic Acids Res*, 28 (2000) 235.

25 Wang Y, Xiao J, Suzek TO, Zhang J, Wang J & Bryant SH, PubChem: a public information system for analyzing bioactivities of small molecules. *Nucleic Acids Res*, 37 (2009) W623.

26 Morris GM, Huey R, Lindstrom W, Sanner MF, Belew RK, Goodsell DS & Olson AJ, Software News and Updates AutoDock4 and AutoDockTools4: Automated Docking with Selective Receptor Flexibility. *J Comput Chem*, 30 (2009) 2785.

27 Sanner MF, The Python interpreter as a framework for integrating scientific computing software components. *J Mol Graph Model*, 26 (2008) 1.

28 O'Boyle NM, Banck M, James CA, Morley C, Vandermeersch T & Hutchison GR, Open Babel: An open chemical toolbox. *J Cheminform*, 3 (2011) 33.

29 Salentin S, Schreiber S, Haupt VJ, Adasme MF & Schroeder M. PLIP: fully automated protein–ligand interaction profiler. *Nucleic Acids Res*, 43 (2015) W443.

30 Ganeshpurkar A, Singh R, Gore PG, Kumar D, Gutti G, Kumar A & Singh SK, Structure-based screening and molecular dynamics simulation studies for the identification of potential acetylcholinesterase inhibitors. *Mol Simul*, 46 (2019) 169.

31 BIOVIA D. S. BIOVIA Discovery Studio Visualizer, v16. 1.0. 15350, San Diego: Dassault Systemes; (2015).

32 Jain S, Sharma S & Sen DJ, Virtual Screening, Docking, ADMET and Molecular Dynamics: A Study to Find Novel Inhibitors of Mycobacterium Tuberculosis Targeting QcrB. *Jordan J Chem*, 16 (2022) 131.

33 Jain S, Sharma S & Sen DJ, An In Silico Study of Imidazo[1, 2-a]Pyridine Derivatives with Homology-Modelled F1F0 ATP Synthase Against Mycobacterium Tuberculosis. *Anti-Infect Agents*, 20 (2022) 81.

34 Azzam KA, SwissADME and pkCSM webservers predictors: An integrated online platform for accurate and comprehensive predictions for in silico ADME/T properties of artemisinin and its derivatives. *KomplIspolz. MinSyra = Compl Use of Min Resour,* 325 (2023) 14.

35 Gandla K, Islam F, Zehravi M, Karunakaran A, Sharma I, Haque MA, Kumar S, Pratyush K, Dhawale SA, Nainu F & Khan SL, Natural polymers as potential P-glycoprotein inhibitors: Pre-ADMET profile and computational analysis as a proof of concept to fight multidrug resistance in cancer. *Heliyon*, 9 (2023) e19454.

36 Sun S, Zhang L, Lu S, Liu H, Yuan H, Chen Y & Lu T, De novo design of PLK1 inhibitors based on 2-amino aromatic heterocyclic scaffold: 3D-QSAR and molecular fragment replacement. *Mol Simul*, 39 (2013) 975.

37 Wiederstein M & Sippl MJ, ProSA-web: interactive web service for the recognition of errors in three-dimensional structures of proteins. *Nucleic Acids Res*, 35 (2007) W407.

38 Mani H, Chang CC, Hsu HJ, Yang CH, Yen JH & Liou JW, Comparison, Analysis, and Molecular Dynamics Simulations of Structures of a Viral Protein Modeled Using Various Computational Tools. *Bioengineering*, 10 (2023) 1004.

39 Paul SK, Metu CLN, Sutihar SK, Saddam M, Paul B, Kabir ML & Helal MMU, A computational investigation on Rho-related GTP-binding protein RhoB through molecular modeling and molecular dynamics simulation study. *bioRxiv,* 2023 (2023) 1.

40 Patel S, Singh VR, Suman AK, Jain S & Sen AK, Virtual Screening, Docking, and Designing of New VEGF Inhibitors as Anti-cancer Agents. *Curr Drug Discov Technol*, 21 (2024) 46.

41 Er-Rajy M, El Fadili M, Imtara H, Saeed A, Ur Rehman A, Zarougui S, Abdullah SA, Alahdab A, Parvez MK & Elhallaoui M, 3D-QSAR studies, molecular docking, molecular dynamic simulation, and ADMET proprieties of novel pteridinone derivatives as PLK1 inhibitors for the treatment of prostate cancer. *Life*, 13 (2023) 127.

42 Tong JB, Luo D, Bian S & Zhang X, Structural investigation of tetrahydropteridin analogues as selective PLK1 inhibitors for treating cancer through combined QSAR techniques, molecular docking, and molecular dynamics simulations. *J Mol Liq*, 335 (2021) 116235.

43 Malkaje S, Srinivasa MG, Deshpande N, Navada S & Revanasiddappa BC, An *In silico* approach: Design, Homology Modeling, Molecular Docking, MM/GBSA Simulations, and ADMET Screening of Novel 1, 3, 4-oxadiazoles as PLK1 inhibitors. *Curr Drug Res Rev*, 15 (2023) 88.

44 Moharana M, Pattanayak SK & Khan F, Identification of phytochemicals from Eclipta alba and assess their potentiality against Hepatitis C virus envelope glycoprotein: Virtual screening, docking, and molecular dynamics simulation study. *J Biomol Struct Dyn*, 41 (2023) 5328.